

Morphological Instability Induced by the Interaction of a Particle with a Solidifying Interface

Layachi Hadji

The University of Alabama, Department of Mathematics, Tuscaloosa, Alabama 35487

(Dated: June 9, 2018)

We show that the interaction of a particle with a directionally solidified interface induces the onset of morphological instability provided that the particle-interface distance falls below a critical value. This instability occurs at pulling velocities that are below the threshold for the onset of the Mullins-Sekerka instability. The expression for the critical distance reveals that this instability is manifested only for certain combinations of the physical and processing parameters. Its occurrence is attributed to the reversal of the thermal gradient in the melt ahead of the interface and behind the particle.

PACS numbers: 81.05.Ni, 81.30.Fb, 81.10.Mx, 81.10.Dn, 81.20.Dn

The freezing of a liquid with a dispersed phase takes place in numerous natural and industrial processes. Some examples include the formation of ice lenses that result from the freezing of soil water [1], the freezing of biological cell suspensions in a cryopreservation experiment [2], the decontamination of metallic pollutants from soils [3], the growth of Y123 superconductors by the undercooling method [4] and the manufacture of particulate reinforced metal matrix composites (PMMC) [5]. The properties of these composite materials are enhanced by the addition of the dispersed elements. The freezing of a liquid suspension is associated with the interaction of the constituents of the dispersed phase with a solidifying interface. The first systematic study of this interaction was carried out by Uhlmann *et al.* [6]. They demonstrated the existence of a critical value for the growth rate below which the inclusions are pushed by the moving interface, and above which they are engulfed by the interface and incorporated into the solid. Consequently, very low growth rates are conducive to particles being pushed by the interface, while high growth rates are conducive to particle engulfment.

The presence of an inclusion in the melt near a solid-liquid interface introduces locally a change, albeit small, in the thermal gradient ahead of the solid front. This, in turn, introduces a small deformation in the profile of the interface. The difference in the thermal conductivities of the melt and particle stands out as the cause for this interfacial deflection [7, 8, 9, 10]. Imagine a situation wherein a solid is growing antiparallel to the direction of the heat flux and toward an inclusion that is less heat conducting than the melt in which it is immersed. Then, as the width of the gap separating the inclusion from the solid front decreases, heat becomes more easily evacuated from the solid phase than from ahead, leading to a local reversal of the thermal gradient and, consequently, to the local destabilization of the interface. As long as the particle remains pushed, the disturbance grows and propagates radially with decreasing magnitude.

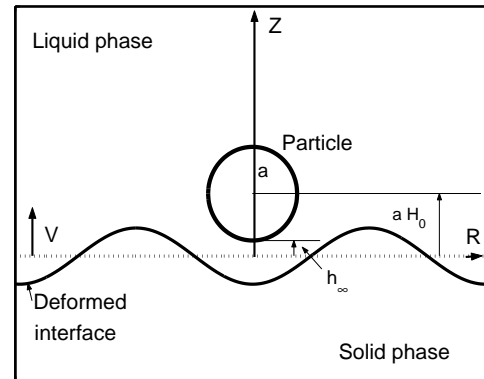


FIG. 1: Sketch of a particle of radius a immersed in a melt near a deformable solid-liquid interface; aH_0 is the particle-interface distance measured from the particle's center to the planar solid front, V is the interface growth rate, h_∞ is the gap width that separates the lowest point on the particle from the planar interface, and R represents the radial coordinate taken along the planar interface.

This hand-waving argument is made more precise in this paper. The situation considered here is illustrated schematically in Fig. 1. An axisymmetric spherical particle of radius a is submerged in a binary alloy in such a way that the distance from its center to the planar solid-liquid interface that emerged from the directional solidification of a dilute binary mixture is aH_0 . We assume a microgravity environment. The problem is described by the diffusion of solute equation in the melt and the heat conduction equations in the melt, solid phase and particle in a frame that is moving with velocity V in the upward Z -direction; Z is the vertical coordinate ($Z > 0$ in the liquid region) and R is the radial coordinate taken along the planar solid-liquid interface. The diffusion of solute in the solid phase is neglected. The boundary conditions at the solid-liquid interface account for: (i) curvature and solute undercoolings in the equation describing the equilibrium temperature, (ii) the heat balance, and (iii) the conservation of mass. At the particle-melt boundary, $[Z - (a + h_\infty)]^2 + R^2 = a^2$, we impose the zero mass flux

and the continuity of the temperature and heat flux; h_∞ denotes the width of the gap between the particle and the planar interface. Far away from the solid front, the imposed thermal gradients in the solid and liquid phases are $G^{(L)}$ and $G^{(S)}$, respectively, while the concentration of solute is maintained at C_∞ . The nondimensionalisation that we adopt makes use of the particle's radius a as length scale [11], a/V , the melting point T_m , the growth rate V , and the concentration far away from the front, C_∞ , as scales for time, temperature, velocity and concentration, respectively. We have

$$\epsilon \left(\frac{\partial C}{\partial t} - \frac{\partial C}{\partial z} \right) = \Delta_r C + \frac{\partial^2 C}{\partial z^2}, \quad (1)$$

$$\epsilon \lambda^{(q)} \left(\frac{\partial T^{(q)}}{\partial t} - \frac{\partial T^{(q)}}{\partial z} \right) = \Delta_r T^{(q)} + \frac{\partial^2 T^{(q)}}{\partial z^2}, \quad (2)$$

where C is the solute concentration, T is the temperature, the superscript (q) stands symbolically for particle ($q = P$), solid ($q = S$) and liquid ($q = L$), $\lambda^{(q)} = D/D^{(q)}$, where D and $D^{(q)}$ are the coefficients of solute and thermal diffusion, respectively, $\epsilon = aV/D$ is the Peclet number, and Δ_r is the Bessel differential operator, $(1/r)\partial/\partial r(r\partial/\partial r)$. The corresponding boundary conditions are as follows: at the solid-liquid interface,

$$T^{(S)} = T^{(L)} = 1 - \sigma\kappa + MC, \quad (3)$$

$$\mathcal{S}v_n = (k\nabla T^{(S)} - \nabla T^{(L)}) \cdot \mathbf{n}_i, \quad (4)$$

$$\epsilon C(1 - K)v_n = -\nabla C \cdot \mathbf{n}_i. \quad (5)$$

At the particle's surface, $(z - H_0)^2 + r^2 = 1$, the continuity of temperature and of the heat flux imply,

$$T^{(L)} = T^{(P)}, \quad (\alpha \nabla T^{(P)} - \nabla T^{(L)}) \cdot \mathbf{n}_P = 0, \quad (6)$$

while the zero mass flux condition yields $\nabla C \cdot \mathbf{n}_P = 0$. The far field conditions are $\partial T^{(L)}/\partial z \rightarrow G_L$ and $C = 1$ as $z \rightarrow \infty$, and $\partial T^{(S)}/\partial z \rightarrow G_S$ as $z \rightarrow -\infty$. The symbols that appear in the above equations are defined as follows: $\sigma = \sigma_{SL}/aL$ is the surface energy parameter, where σ_{SL} is the interface excess free energy and L is the latent heat of fusion per unit volume; $M = mC_\infty/T_m$, is the morphological parameter, where m is the liquidus slope; $\mathcal{S} = LVa/(T_m k^{(L)})$ is the Stefan number; $k = k^{(S)}/k^{(L)}$; $\alpha = k^{(P)}/k^{(L)}$, where $k^{(q)}$ is the coefficient of thermal conductance; K is the segregation coefficient; v_n is the normal growth velocity; \mathbf{n}_i and \mathbf{n}_P are the unit normal vectors pointing into the melt at the interface and particle's surface, respectively; $G_L = aG^{(L)}/T_m$ and $G_S = aG^{(S)}/T_m$, where $G^{(q)}$ is the imposed (dimensional) thermal gradient, and κ is the curvature taken to be positive when the center of

curvature lies in the solid phase.

The above set of equations (with $\epsilon = 0$) [12] admits a base state with a planar interface growing at constant speed. The determination of the thermal fields in an infinite medium in which a spherical inclusion has been embedded has been carried out [13]. Here, we make use of the method of images [14] to calculate the thermal fields in the melt and particle that satisfy the equilibrium temperature condition at the planar interface, Eq. (3), and the conditions at the particle's surface, Eq. (6). Then an expression for the thermal field in the solid is derived. This expression must satisfy the temperature condition at the planar interface, Eq. (3), and must also support a planar interface growing with constant speed, Eq. (4). We have

$$C_B(r, z) = 1, \quad \text{in the melt}, \quad (7)$$

$$T_B^{(L)}(r, z) = 1 + G_L z + M + U(r, z), \quad \text{in the melt}, \quad (8)$$

$$T_B^{(S)}(r, z) = 1 + G_S z + M + \frac{U(r, z)}{k}, \quad \text{in the solid}, \quad (9)$$

$$T_B^{(P)}(r, z) = \frac{3G_L z}{2 + \alpha} + 1 + M, \quad \text{in the particle}. \quad (10)$$

where

$$U(r, z) = G_L \left(\frac{1 - \alpha}{2 + \alpha} \right) \sum_{\substack{n=-\infty \\ n \neq 0}}^{\infty} \frac{z + nH_0}{[(z + nH_0)^2 + r^2]^{3/2}}. \quad (11)$$

The plot of the basic profile for the melt's temperature, Eq. (8), is shown in Fig. 2. It pertains to an axisymmetric particle of radius $a = 10\mu\text{m}$ whose center is on the z -axis and whose separation from the interface is $0.5\mu\text{m}$. It depicts an unstable configuration, wherein the thermal gradient in the gap is reversed due to the thermally insulating character of the particle. The configuration is, however, stable for the case of a highly conducting particle.

In order to examine the stability of the base state, we first superimpose axisymmetric, time-dependent infinitesimal disturbances $\theta^{(q)}$, c and η upon the basic state solutions $T_B^{(q)}$, C_B , and the planar interface, respectively. We let

$$[T^{(q)}, C] = [T_B^{(q)}, C_B] + \epsilon[\theta^{(q)}, c], \quad (12)$$

in Eqs. (1)-(6). The resulting equations are then linearized with respect to the disturbances. The following perturbed problem is obtained,

$$\Delta_r \theta^{(q)} + \frac{\partial^2 \theta^{(q)}}{\partial z^2} = -\lambda^{(q)} \frac{\partial T_B^{(q)}}{\partial z}, \quad (13)$$

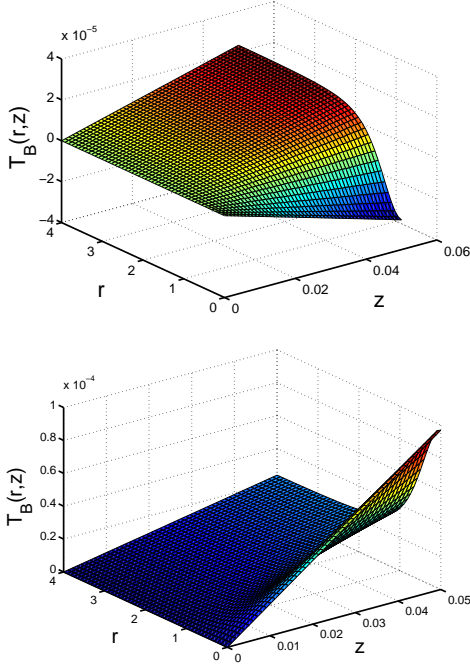


FIG. 2: Plot of the basic temperature profile in the melt (Eq. (8)) for a particle of radius $a = 10\mu m$, dimensionless gap thickness $h_\infty/a = 0.05$ and thermal conductance ratios $\alpha = 0$ (left) and $\alpha = 10$ (right). Note the reversal in the temperature gradient in the gap separating the particle from the interface for the insulating particle case. The profile is evaluated using parameter values for a succinonitrile-acetone system (SCN-ACE) [15, 16].

$$\Delta_r c + \frac{\partial^2 c}{\partial z^2} = 0, \quad (14)$$

$$\theta^{(L)} = -G_L \eta + \sigma \Delta_r \eta - F(r) \eta + M c, \quad z = 0, \quad (15)$$

$$\theta^{(S)} = -G_S \eta + \sigma \Delta_r \eta - \frac{F(r)}{k} \eta + M c, \quad z = 0, \quad (16)$$

$$\frac{\partial c}{\partial z} = K - 1, \quad z = 0, \quad (17)$$

$$S \frac{\partial \eta}{\partial t} = k \frac{\partial \theta^{(S)}}{\partial z} - \frac{\partial \theta^{(L)}}{\partial z}, \quad (18)$$

where the small slope approximation has been invoked in the expression for the curvature, $\kappa \approx -\Delta_r \eta$, where η is the perturbation of the planar position, and

$$F(r) = \frac{\partial U}{\partial z}(r, 0) = 2G_L \left(\frac{1 - \alpha}{2 + \alpha} \right) \sum_{n=1}^{\infty} \frac{r^2 - 2(nH_0)^2}{[r^2 + (nH_0)^2]^{5/2}}. \quad (19)$$

The far field conditions for the perturbations are zero concentration and zero thermal gradients in the liquid and solid phases. The stability problem is solved using the finite Hankel transform over the range $[0, \ell]$ [17]. On using the approximation $F(r) \sim F(0)$ as $r \rightarrow 0$, we find

$$\hat{\theta}^{(L)} = \left[-[G_L + \sigma \omega^2 + \frac{2\zeta(3)(\alpha - 1)}{(2 + \alpha)H_0^3} G_L] \hat{\eta} + M \frac{\ell(1 - K)}{\omega^2} J_1(\omega \ell) - \lambda^{(L)} L(\omega) \right] e^{-\omega z} + \lambda^{(L)} L(\omega), \quad (20)$$

$$\hat{\theta}^{(S)} = \left[-[G_S + \sigma \omega^2 + \frac{2\zeta(3)(\alpha - 1)}{k(2 + \alpha)H_0^3} G_L] \hat{\eta} + M \frac{\ell(1 - K)}{\omega^2} J_1(\omega \ell) - \lambda^{(S)} L(\omega) \right] e^{\omega z} + \lambda^{(S)} L(\omega), \quad (21)$$

$$L(\omega) = \frac{\ell G_L J_1(\omega \ell)}{\omega^3} + \frac{1}{\omega^2} \int_0^\ell F(r) r J_0(\omega r) dr, \quad (22)$$

where the hat symbol indicates transformed variables, ω is the wavenumber, J_m is the Bessel function of the first kind of order m and ζ stands for the zeta function, i.e. $\zeta(3) = \sum_{n=1}^{\infty} n^{-3}$.

On imposing the heat balance equation at the interface, Eq. (18), an evolution equation for the growth of

the perturbation $\hat{\eta}$ is obtained. Its solution yields,

$$\hat{\eta}(t) = \frac{g(\omega)}{\Lambda(\omega)} + [\hat{\eta}(0) - \frac{g(\omega)}{\Lambda(\omega)}] e^{-\Lambda(\omega)t/S}, \quad (23)$$

where

$$\Lambda(\omega) = \frac{\omega}{S} \left[\mathcal{G} + (1 + k) \sigma \omega^2 + \frac{4\zeta(3)(\alpha - 1)G_L}{(2 + \alpha)H_0^3} \right], \quad (24)$$

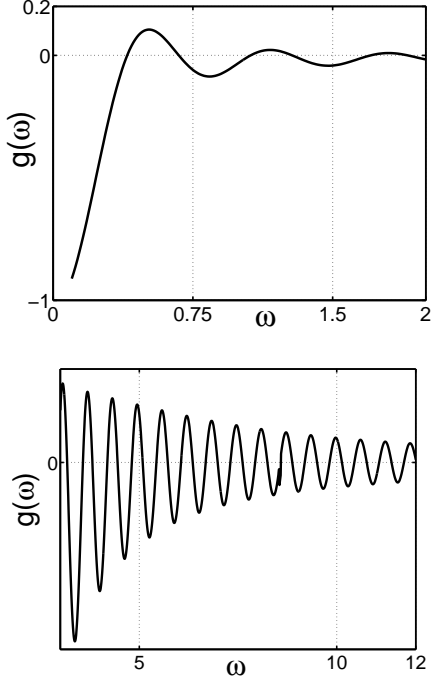


FIG. 3: The small wavenumber behavior (left) and the large wavenumber behavior (right) of the function $g(\omega)$ for a system consisting of SCN-ACE containing silicon-carbide (SiC) particles. The numerical values of the physical constants are [15, 16]: liquidus slope $m = -2.8 \text{ K/wt\%}$, segregation coefficient $K = 1$, $C_\infty = 1.3 \text{ Wt\%}$, melting point $T_m = 328 \text{ K}$, coefficients of thermal conductivity $k^{(P)} = 85 \text{ Wm}^{-1}\text{K}^{-1}$, $k^{(S)} = 0.225 \text{ Wm}^{-1}\text{K}^{-1}$ and $k^{(L)} = 0.223 \text{ Wm}^{-1}\text{K}^{-1}$ for the particle, solid and liquid, respectively; thermal gradients $G^{(S)} = 8000 \text{ Km}^{-1}$ and $G^{(L)} = 10800 \text{ Km}^{-1}$ in the solid and liquid, respectively; $\sigma_{sl} = 0.009 \text{ Jm}^{-2}$; H_0 and ℓ have been arbitrarily chosen to equal 1.1 and 10, respectively; $L = 4.6 \times 10^7 \text{ Jm}^{-3}$.

$$g(\omega) = M(1+k)\ell(1-K)\frac{J_1(\omega\ell)}{\omega S} - \frac{\lambda\omega L(\omega)}{S}, \quad (25)$$

$\mathcal{G} = kG_S + G_L$ is the conductivity weighted thermal gradient, and $\lambda = \lambda^{(S)} + \lambda^{(L)}$. The conditions for marginal stability are determined by setting the growth rate to zero, i.e. $\Lambda(\omega) = 0$. However, when $\Lambda = 0$, the term $g(\omega)/\Lambda(\omega)$ in Eq. (23) is undefined. Therefore, no meaning to the dispersion relation, $\Lambda(\omega) = 0$, could exist if ω did not satisfy the auxiliary equation $g(\omega) = 0$. The ratio, $g'(\omega)/\Lambda'(\omega)$, where $\iota = d/d\omega$ is however finite. The function $g(\omega)$ is singular at $\omega = 0$ and has infinitely many zeros ω_j , $j = 1, 2, 3, \dots$, on the positive ω -axis (Fig. 3). We set $\omega = \omega_j$ in the dispersion relation $\Lambda(\omega) = 0$ and solve for H_0 . The critical value of the particle-interface separation, d_c , is the largest value of H_0 and is obtained by setting ω_j equal to the smallest root ω_1 . We find

$$d_c = \left[\frac{4\zeta(3)(1-\alpha)G_L}{(2+\alpha)[\mathcal{G} + (1+k)\sigma\omega_1^2]} \right]^{1/3}. \quad (26)$$

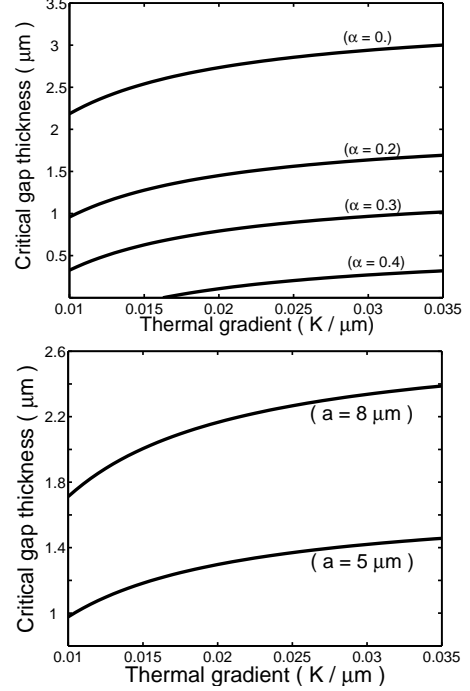


FIG. 4: (left) Plot of the dimensional critical gap thickness, $(d_c - 1)a$, as function of the dimensional thermal gradient in the melt, $G^{(L)}$, in unit of Kelvin per micrometer for selected values of the thermal conductance ratio α , (right) plot of the critical gap thickness for 2 insulating particles of radii $5 \mu\text{m}$ and $10 \mu\text{m}$ as function of the imposed thermal gradient in the melt $G^{(L)}$.

Equation (26) describes the instability criterion in terms of dimensionless terms. It implies that for prescribed thermal gradients in the liquid and solid, and for a given thermal conductance ratio α , instability of the planar interface sets in whenever the dimensionless distance from the particle's center to the interface, measured by H_0 , equals d_c . From the physical standpoint, the instability is manifested only for parameter values for which d_c exceeds unity and the expression $(1-\alpha)G_L$ is positive. Figure 4 depicts the range of parameters for which the instability is observable for a system consisting of SCN-ACE that is immersed with particles of different sizes and thermal conductivities. The plot of the dimensional critical gap thickness, $h_\infty = (d_c - 1)a$, as a function of the thermal gradient in the melt, $G^{(L)}$, for particles of different thermal conductivities show that the critical gap thickness (i) increases with $G^{(L)}$, (ii) decreases with α , and (iii) particles characterized by high values of α require high thermal gradients for the instability to set in. For increasing particle's size, the critical gap thickness increases as α and $G^{(L)}$ remain constant. Furthermore, we note that the onset of the instability, being of thermal origin, does not depend explicitly on the concentration. However, the magnitude of d_c is affected by the morphological number due to the dependence of the auxiliary function $g(\omega)$, and thus of the root ω_1 , on M . Depend-

ing on the physical process under consideration, the presence or absence of this instability can be imposed by the selection of an appropriate set of physical parameters as dictated by Eq. (26) and shown in Fig. 4. The instability put forth in this paper also demonstrates the influence a tiny impurity in the melt can have on the morphological stability of the interface.

Ahuja [18] has carried out a detailed experimental study of the influence of foreign particles on the morphology of a slowly growing solid-liquid interface under normal

gravity conditions (see also [19]). These experiments depict *in situ* the real time evolution of the solid-liquid interface shape profile in the vicinity of a single particle. The sequence of photographs depicting the interaction of polystyrene particles in SCN with an initially planar solid-liquid interface, shown on page 101 of Ref. [18], provides qualitative confirmation of the features of the instability put forth in this paper. The quantitative validation of our prediction requires carefully controlled experiments in a microgravity environment.

-
- [1] K.A. Jackson and B. Chalmers, *J. Appl. Phys.* **29**, 1178 (1958).
- [2] H. Ishiguro and B. Rubinsky, *Cryobiology* **31**, 483 (1994).
- [3] G. Gay and M.A. Azouni, *Crystal Growth & Design* **2**, 135 (2002).
- [4] A. Endo, H.S. Chauhan, T. Egi and Y. Shiohara, *J. Mater. Sci.* **11**, 795 (2002).
- [5] A.R. Kennedy and T.W. Clyne, *Cast Metals* **4**, 160 (1991).
- [6] D.R. Uhlmann, B. Chalmers and K.A. Jackson, *J. Appl. Phys.* **35**, 2986 (1964).
- [7] A.M. Zubko, V.G. Lobanov and V.V. Nikonova, *Sov. Phys. Crystallgr.* **18**, 239 (1973).
- [8] A.A. Chernov, D.E. Temkin and A.M. Mel'kinova, *Sov. Phys. Crystallogr.* **22** 656-658 (1977).
- [9] S. Sen, W.F. Faulker, P. Curreri and D.M. Stefanescu, *Met. Trans. A* **28**, 2129 (1997).
- [10] L. Hadji, *Phys. Rev. E* **64**, 051502 (2001).
- [11] The directional solidification of an alloy is subject to a morphological Mullins-Sekerka instability when the growth rate V exceeds some critical value (W.W. Mullins and R.F. Sekerka, [*J. Appl. Phys.* **34**, 323 (1963)]). The planar interface undergoes a bifurcation to a cellular state whose wavelength is determined from a competition between the destabilizing diffusion length scale and the stabilizing capillary length scale. The wavelength varies roughly between 10 and 100 μm . (I. Durand, K. Kassner, C. Misbah and H. Müller-Krumbhaar, [*Phys. Rev. Lett.* **76**, 3013 (1996)]). This wavelength is of the same order of magnitude as the size of the inclusions that are used in PMMC and found in other processes. In this paper, the mere presence of the particle in the melt provides the length scale. Furthermore, the growth rates considered here are so low ($\epsilon \ll 1$) that the Mullins-Sekerka instability does not arise.
- [12] Typically, the size of the inclusions vary between 5 μm and 100 μm , and $D \approx 10^{-9} \text{m}^2\text{s}^{-1}$. We have considered here very low growth rates so that the onset of the Mullins-Sekerka instability is remote and the particle remains pushed by the interface. Thus, for $V \approx 10^{-9} \text{ms}^{-1}$, we have $\epsilon \approx 10^{-5}$. We assume that the perturbation to the interface profile is of order (ϵ). The case of a pure substance with zero growth rate has been analyzed by L. Hadji, [*Scripta Materialia* **48**, 665 (2003)].
- [13] H.S. Carslaw and J.C. Jaeger, *Conduction of Heat in Solids*, second edition (Clarendon Press, Oxford, 1959).
- [14] H. Cheng and L. Greengard, *SIAM J. Appl. Math.*, **58**, pp. 122-141 (1998).
- [15] W. Kurz and D.J. Fisher, *Fundamentals of Solidification*, third edition (Trans. Tech. Publications, Switzerland, 1992).
- [16] D. M. Stefanescu, R.V. Phalnikar, H. Pang, S. Ahuja, and B. K. Dhindaw, *SIJ Int.* **35**, 300 (1995).
- [17] A.D. Poularikas, *The Transforms and Applications Handbook*, second edition (CRC Press, Boca Raton, Florida, 1999). The interaction of a single particle with the interface sets up a perturbation in the interface due to the difference in thermal conductivities ($\alpha \neq 1$). In case the instability sets in, this disturbance travels radially in all directions, decreasing in magnitude as it goes. Far away from the particle, at $r = \ell$, the particle's effect vanishes. In our calculations, we have arbitrarily chosen $\ell = 10$.
- [18] S. Ahuja, Ph.D. Dissertation, The University of Alabama, p. 100 (1992).
- [19] J.A. Sekhar and R. Trivedi, *Mater. Sci. Eng. A* **147**, pp. 9-21 (1991). This paper investigates the morphological stability of a solidifying interface in the presence of large number of particles.